Journal of Organometallic Chemistry 915 (2020) 121235

Contents lists available at ScienceDirect

Journal of Organometallic Chemistry

journal homepage: www.elsevier.com/locate/jorganchem

Carbene complex formation versus cyclometallation from a phosphoryl-tethered methanide ruthenium complex

Kai-Stephan Feichtner, Florian Papp, Michelle Schmidt, Maurice Paaßen, Viktoria H. Gessner*

Faculty of Chemistry and Biochemistry, Chair of Inorganic Chemistry II, Ruhr University Bochum, Universitätsstr. 150, 44801, Bochum, Germany

ARTICLE INFO

Article history:
Received 31 January 2020
Received in revised form
12 March 2020
Accepted 14 March 2020
Available online 19 March 2020

Dedicated to Prof. Dr. Ekkehardt Hahn on the Occasion of his 65th Birthday.

Keywords:
Carbene complex
Cyclometallation
C–H activation
DFT studies

ABSTRACT

An oxophosphoryl-substituted methanide ligand system for transition metal complexes has been synthesized and isolated as the sodium salt Na[$Ph_2P(O)–C(H)–SO_2Ph$]. This ligand features structural components known to enable the isolation of nucleophilic late transition metal carbene complexes. The corresponding ruthenium(cymene) chlorido complex was readily available by simple salt metathesis reaction. However, in contrast to previously reported thio- and iminophosphoryl-tethered ligand systems, dehydrohalogenation of the chlorido complex led to the formation of a cyclometallated ruthenium complex instead of the carbene complex. All compounds have been characterized in solution and solid state. Additional density functional theory (DFT) studies have been performed to elucidate the mechanism of the observed cyclometallation and to shed light on the effects of different P(V) groups in the ligand system on the stability and reactivity of the corresponding carbene complexes. The calculations show that the weaker coordination of the P=O compared to the P=S or P=N moiety is responsible for the more facile C–H activation.

© 2020 Elsevier B.V. All rights reserved.

1. Introduction

Methandiide-derived carbene complexes have received intense research interest over the past two decades. Since the pioneering work by Cavell and coworkers [1] these systems were found to be versatile ligands for the preparation of nucleophilic carbene complexes with metals covering the whole periodic table, including nucleophilic actinide and late transition metal carbenes [2,3]. The latter showed promising properties for applications in bond activation reactions via metal ligand cooperation (MLC) [4] involving the M = C linkage and hence in catalytic transformations. For example, the thiophosphoryl-tethered ruthenium carbene complex **2** which is readily available from dilithium methandiide **1** is able to activate a series of element hydrogen bonds of different polarity (O–H, P–H, H–H, Si–H, B–H; Scheme 1) also in a reversible fashion [5,6].

In order to optimize the ligand design in such carbene species for MLC our group has focused on the variation of the substitution pattern at the carbene carbon atom to tune the electronics of the M = C interaction and thus the thermodynamics of the bond activation processes [7]. To date, almost all methandiide-derived carbene complexes feature P(V) moieties for stabilization, most of which are imino or thiophosphoryl side-arms [3,8]. These side-arms are necessary to increase the complex stability, but also influence the electronics of the metal and thus the metal carbon linkage [9]. For example, strong donor groups render the metal more electron-rich and thus hamper sufficient electron transfer from the methandiide ligand to the metal. This typically results in a highly polar, ylidic M – C interaction with a highly nucleophilic carbon atom. In contrast, electron-accepting co-ligands make the metal more acidic and thus result in a more covalent M = C double bond. Hence, the propensity of the M = C bond to undergo 1,2 addition reactions can be influenced by variation of the donor groups. For example, we recently demonstrated that the exchange of the thiophosphoryl group in **1** by an iminophosphoryl moiety P=NTMS changes the selectivities in B–H bond activation reactions [5f] and also influences the polarity and thus reactivity of the corresponding carbene complexes [7e].

Since weaker electron-donating groups lead to less polarized M = C double bonds they in general facilitate reversible activation processes and should thus be beneficial for realizing catalytic processes. In this context, we aimed for the synthesis of an oxo-

* Corresponding author.
E-mail address: viktoria.gessner@rub.de (V.H. Gessner).

https://doi.org/10.1016/j.jorganchem.2020.121235
0022-328X/© 2020 Elsevier B.V. All rights reserved.

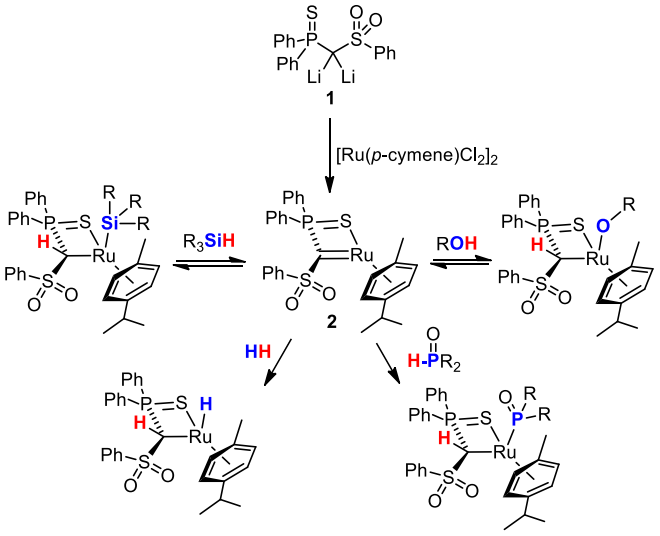

Scheme 1. Synthesis of methandiide-derived carbene complex **2** and its application in bond activations.

phosphoryl substituted ruthenium carbene complex in order to further examine the influence of the donor strength of stabilizing groups on the behavior and reactivity of the carbene complexes.

2. Results and discussion

The synthesis of phosphine oxide **3** was accomplished by a similar procedure as reported by Imamoto et al. involving the lithiation of methyl phenyl sulfone followed by the addition of tri-*iso*-butylaluminum to form the corresponding alanate [10]. Reaction with chlorodiphenylphosphine and subsequent oxidation delivered the phosphine oxide in 61% yield as colorless solid (for crystal structure see the SI and Table 1). Transmetallation from lithium to aluminum was necessary to reduce the formation of the diphosphorylated compound. While double metalation of **3** turned out to be difficult, the monodeprotonation can easily be accomplished with sodium hydride in THF at room temperature (Scheme 2). Treatment of the ligand with 1 equiv. of base selectively resulted in the formation of sodium methanide **3-Na**, which was isolated as colorless solid in an excellent yield of 93%. **3-Na** is characterized by a signal at 19.7 ppm in the $^{31}P\{^{1}H\}$ NMR spectrum (20.4 ppm [7a] for **3**). The ^{1}H NMR spectrum shows broadened signals indicating the formation of oligo- or polymeric structures in solution as it has been observed for other phosphoryl-stabilized methanides. The presence of 0.75 equivalents of THF in the NMR spectra even after prolonged drying of the solid in vacuum suggests the coordination of THF to the oligomeric species [11]. The hydrogen atom at the methanide carbon atom gives rise to a broadened multiplet at 2.58–2.64 ppm. The methanide carbon atom appears at 47.9 ppm

Table 1
Comparison of important bond lengths and angles in **3**, **3-Na**, **4** and **5**.

Bond [Å][a] Angle [°]	3	3-Na	4	5
P1–C1	1.824(2)	1.724(3)	1.7842(19)	1.782(3)
S1–C1	1.782(2)	1.674(3)	1.7495(18)	1.741(3)
P1–O3	1.4858(16)	1.499(2)	1.5230(14)	1.523(2)
S1–O[a]	1.4373(24)	1.450(4)	1.4456(21)	1.451(4)
Ru1–C1	–	–	2.2163(18)	2.149(3)
P1–C1–S1	118.80(13)	119.50(16)	121.14(11)	120.08(19)

[a] Average values.

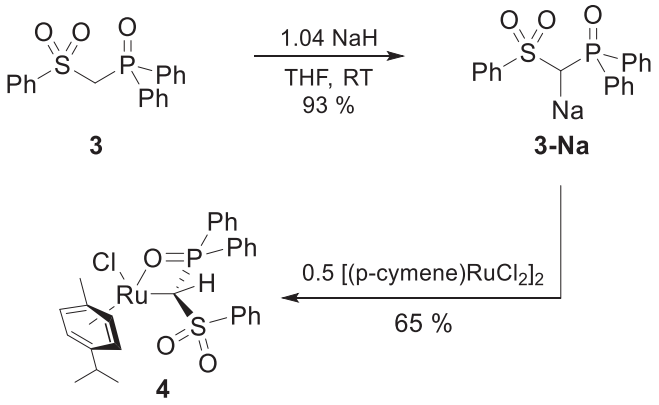

Scheme 2. Synthesis of **3-Na** and ruthenium complex **4**.

with a large coupling constant of $^{1}J_{PC}$ = 129.8 Hz in the $^{13}C\{^{1}H\}$ NMR spectrum.

Single crystals of **3-Na** were obtained by addition of 15-crown-5 and diffusion of *n*-pentane into a saturated THF solution. **3-Na**·(15-crown-5) crystallizes as monomer in the monoclinic space group $P2_1$ (Fig. 1). The asymmetric unit contains two molecules of the complex, which show similar bond length and angles. Therefore, only bond lengths and angles for the molecule shown in Fig. 1 will be discussed. In the structure, the sodium ion is coordinated by the crown ether as well as the phosphoryl and sulfonyl group. No contact to the methanide carbon atom is observed, which has often been reported for analogous phosphoryl and sulfonyl functionalized monoanions [11,12]. The central carbon atom is slightly pyramidalized with a sum of angles of 355.5(20)°, which still accounts for a lone pair at carbon with mainly p-character (in the second molecule in the asymmetric unit, the sum of angles amounts to

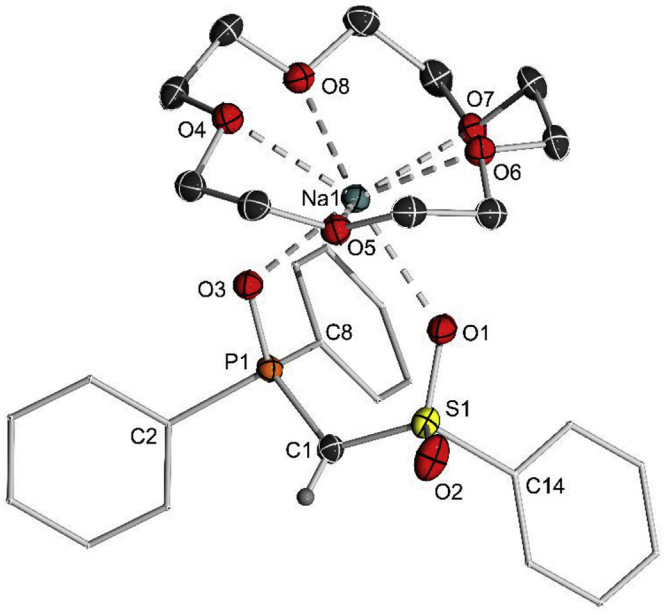

Fig. 1. Molecular structure of **3**-Na·(15-crown-5). Only one molecule of the asymmetric unit is shown. Ellipsoids drawn at the 50% probability level. Hydrogen atoms (except for the methylene bridge) omitted for clarity. Selected bond lengths [Å] and angles [°]: C1–P1 1.724(3), C1–S1 1.674(3), P1–O3 1.499(2), P1–C2 1.820(3), P1–C8 1.822(3), S1–O1 1.458(2), S1–O2 1.441(2), S1–C14 1.789(3), O1–Na1 2.412(2), O3–Na1 2.280(2), Na1–O4 2.546(2), Na1–O5 2.494(2), Na1–O6 2.536(2), Na1–O7 2.438(2), Na1–O8 2.450(2), P1–C1–S1 119.53(18).

360.1(30)). The S1–C1 distance of 1.674(3) Å and the P1–C1 distance of 1.724(3) Å in the central structural motive are considerable shorter than in the protonated precursor (1.782(2) and 1.824(2) Å in **3**), thus reflecting the increasing charge at the central carbon atom and the resulting electrostatic interactions within the PCS linkage. Because of the stabilization of the carbon lone pair by negative hyperconjugation, the P–O and S–O distances are slightly elongated in **3-Na** compared to **3**.

In order to synthesize the ruthenium carbene complex analogous to **2** a step-wise approach from **3-Na** via salt metathesis by treatment with $[(p\text{-cymene})RuCl_2]_2$ and subsequent dehydrohalogenation was chosen. A direct approach via the corresponding methandiide ligand was not possible, since in contrast to **1** dilithiation of **3** was found to be difficult [13]. Formation of the chlorido complex **4** turned out to be straight-forward. After work-up **4** was isolated as orange solid in 65% yield (Scheme 2). Compared to **3-Na** the phosphorus signal in **4** experiences a remarkable down-field shift, resonating at 68.3 ppm in the $^{31}P\{^1H\}$ NMR spectrum. The methanide proton appears in the ^1H NMR spectrum as a doublet at 3.81 ppm with a coupling constant of $^2J_{HP} = 2.40$ Hz, while the carbon atom gives rise to a doublet at 43.3 ppm with a coupling constant of $^1J_{PC} = 54.4$ Hz in the $^{13}C\{^1H\}$ NMR spectrum. The decreased coupling constant in **4** compared to **3-Na** clearly reflects the higher p-character in the P–C bond which is well in line with the formation of a C–Ru bond. Single-crystals of **4** were obtained by diffusion of *n*-hexane into a saturated solution of **4** in toluene. The ruthenium complex crystallizes in the triclinic space group *P*-1. The asymmetric unit contains two molecules of **4** as well as a pentane molecule on the symmetry centre (Fig. 2). Discussion will be conducted on only one moiety of **4** since both molecules in the asymmetric unit show similar bond lengths and angles. The structure confirms the formation of the expected chlorido complex, in which the methanide acts as a C,O-ligand coordinating via the phosphoryl moiety. The Ru–C bond length of 2.2163(18) Å is well in line with a Ru–C single bond [5b]. Due to the formation of the Ru–C bond and the reduced negative charge at the methanide carbon atom compared to **3-Na**, the P–C and C–S distances are longer than in the sodium compound, but are still slightly shorter than in the ligand itself (see Table 1).

Next, the dehydrohalogenation of **4** was attempted with *tert*-butoxide bases. Monitoring of the reaction process by $^{31}P\{^1H\}$ NMR spectroscopy revealed the slow formation of two new products with signals at approximately $\delta_P = 75.6$ ppm and 60.9 ppm (Scheme 3). During the course of the reaction, the signal at $\delta_P = 75.6$ ppm completely vanished, thus exclusively giving way to a compound with a phosphorus shift of $\delta_P = 60.9$ ppm. Isolation revealed the product to be the cyclometallated complex **5** instead of the desired carbene complex **6.** After 2 h of reaction time approximately 60% of the starting material was consumed. Full conversion was only achieved after five days. We assume, that the interim observed peak at 75.6 ppm corresponds to the desired carbene complex **6**. Due to the slow deprotonation an isolation or trapping of the carbene species was not possible. It is also possible, that the observed intermediate is a compound with a cyclometallated phosphorus bound phenyl ring which then further converts to the isolated product **5** (see compounds **8′** and **9′** in the SI 4.1.6, Scheme S2). **5** was isolated as orange solid in 55% yield and characterized by multi-nuclear NMR spectroscopy, elemental and XRD analysis. Although such a cyclometallation was not observed for the thiophosphoryl-tethered carbene complex **2**, analogous reactions have been reported for other nucleophilic carbene complexes [14].

The crystal structure of **5** unambiguously confirms the cyclometallation of the sulfur bound phenyl group (see Fig. 3). The ruthenium centre adopts a piano-stool geometry with an "open-book"-shaped structure of the methanide ligand. The bond lengths in the methanide ligand in **5** are similar to those found in the starting complex **4**. The most significant difference concerns the Ru–C bond (2.149(3) Å), which is – probably due to the rigid *C,C,O*-coordination mode of the ligand – slightly shorter in the cyclometallated complex.

The facile cyclometallation to **5** is in contrast to the related thio- or iminophosphoryl systems, which could both be isolated as stable solids at room temperature [5b,7e]. The instability of the P=O substituted carbene complex is presumably the result of the weak coordination of the phosphoryl moiety to ruthenium and/or the polarity of the Ru–C double bond in carbene complex **6**. In order to better understand the reason for the low stability of carbene complex **6**, we performed computational studies at the PBE0/def2tzvp level of theory. A model system with *p*-xylene instead of a *p*-cymene ligand was used to prevent calculations of multiple possible conformers.

At first, natural bond orbital (NBO) analyses [15] of carbene complex **6′** in comparison to complex **2′** were carried out on the PBE0/def2tzvp (ECP MWB28 for Ru) level of theory to probe the impact of the oxophosphoryl-tether on the electronics of the M = C bond (Fig. 4). These calculations revealed, that the exchange of the thiophosphoryl moiety by an oxophosphoryl group only leads to a minor change of the polarity of the Ru=C double bond. In fact, the double bond is slightly less polar in complex **6′** which should lead to an overall more stable carbene complex. Likewise, the Wiberg bond index of the Ru=C bond is slightly higher in **6′** than in **2'**. Therefore, the low stability of complex **6′** compared to **2′** cannot be explained by a higher reactivity of the Ru=C double bond due to an increased polarity [16].

Next, we turned our attention towards the mechanism of the

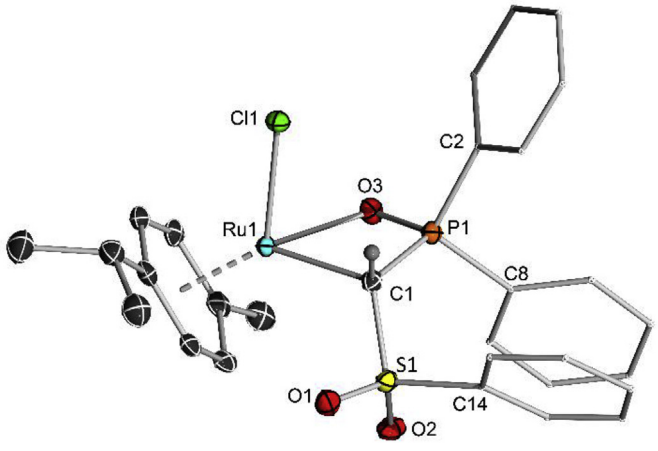

Fig. 2. Molecular structure of **4**. Only one molecule of the asymmetric unit shown. Ellipsoids drawn at the 50% probability level. Hydrogen atoms (except for the methylene bridge) omitted for clarity. Selected bond lengths [Å] and angles [°]: C1–S1 1.7495(18), C1–P1 1.7842(19), C1–Ru1 2.2163(18), S1–O1 1.4460(15), S1–O2 1.4452(14), S1–C14 1.7822(19), P1–O3 1.5230(14), P1–C2 1.7931(19), P1–C8 1.801(2), O3–Ru1 2.1654(13), Ru1–Cl1 2.4090(4), S1–C1–P1 121.14(11).

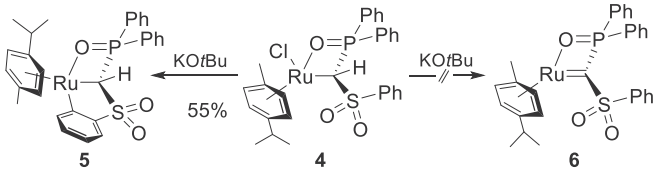

Scheme 3. Synthesis of complex **5** from **4**.

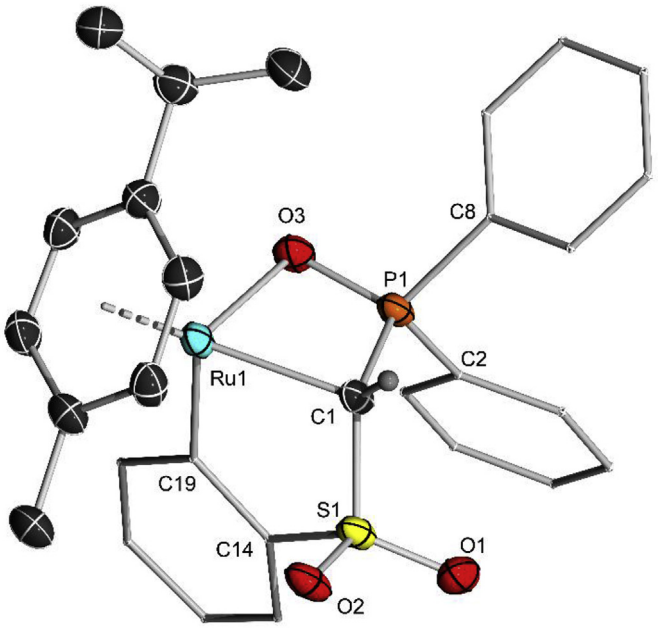

Fig. 3. Molecular structure of **5**. Ellipsoids drawn at the 50% probability level. Hydrogen atoms (except for the methylene bridge) omitted for clarity. Selected bond lengths [Å] and angles [°]: C1–S1 1.741(3), C1–P1 1.782(3), C1–Ru1 2.149(3), P1–O3 1.523(2), P1–C8 1.797(3), P1–C2 1.801(3), S1–O1 1.446(3), S1–O2 1.455(2), S1–C14 1.758(3), C19–Ru1 2.070(3), Ru1–O3 2.232(2), S1–C1–P1 120.08(19).

orthometallation of the P═O- in comparison to the P═S-substituted carbene complex **2**. Due to the analogy of both ligands we assumed that also the oxophosphoryl ligand first allows the formation of the carbene complex, from which onwards cyclometallation occurs. Different reaction pathways, particularly for the start of the reaction were calculated. Only the energetically most favorable pathway is shown in Scheme 4 and discussed here (see the experimental section for details). The reaction starts with the additional coordination of the sulfonyl moiety via an oxygen atom to the ruthenium centre. This coordination is accompanied by a change from a Ru═C double to a Ru–C single bond and a pyramidalization of the former carbene carbon atom. A similar flexible behavior of the metal carbon bond which enabled the activation of small molecules via oxidative addition due to the opened coordination site has been observed in a methandiide-derived iridium carbene complex [7d]. The calculated bond lengths for the metal carbon bond in **2'** (1.927 Å), **6'** (1.908 Å) and **Int1** (X = S: 2.192 Å; X = O: 2.205 Å) are well in line with reported ruthenium carbon double and single bonds [5b]. Starting from **Int1**, decoordination of the P = X moiety and reformation of the Ru═C double bond leads to the intermediates **Int2(S)** and **Int2(O)**, respectively. Both intermediates are energetically disfavored ($\Delta G^{\ddagger}$ = 52.5 kJ/mol and 11.4 kJ/mol respectively) albeit this is more pronounced for the thiophosphoryl-substituted system as expected due to the stronger donor ability of the P═S-moiety. The transition state **TS-2** in this reaction step is the crucial part of the mechanism since the relative free energy amounts to $\Delta G^{\ddagger}$ = 130.6 kJ/mol for the thiophosphoryl-substituted system and to 93.0 kJ/mol for the oxophosphoryl-substituted compound. This explains why the orthometallation takes place at room temperature only for the oxophosphoryl-functionalized carbene complex. After rotation around the C–S bond leading to 18 valence electrons intermediate **Int3** with an agostic ruthenium C–H-interaction, the oxidative addition/C–H activation takes place resulting in intermediate **Int4**. These two steps are energetically considerably disfavored and represent the steps with the highest activation barrier in the whole reaction sequence. However, subsequent proton transfer is facile and recoordination of the phosphoryl moiety gives the energetically favoured orthometallated compounds **5'** (ΔG = −70.9 kJ/mol) and **6'** (ΔG = −57.9 kJ/mol) respectively. It is important to note, that the highest barrier in the whole cyclometallation mechanism is considerably higher for the thiophosphoryl compound (**TS-4(S)**, $\Delta G^{\ddagger}$ = 154.8 kJ/mol) than for the oxophosphoryl complex. The latter features a maximum barrier of 106.0 kJ/mol, which is still low enough for the reaction to proceed at room temperature, while complex **2** is stable towards cyclometallation due to the highly disfavored decoordination of the P═S group from the ruthenium centre. This is in line with observations by Mézailles and coworkers with a PS/PO methanide ligand [14b]. Overall the calculations confirm the experimental results and show, that the weaker donor ability of the oxophosphoryl moiety compared to the thiophosphoryl moiety enables the decoordination of the phosphonium group and thus allows for a more facile oxidative addition of an ortho-standing C–H bond at the ruthenium centre. We would like to point out that the weaker coordination ability of the oxophosphoryl group is also reflected in the WBIs depicted in Fig. 4, which is clearly lower for the Ru–O than for the Ru–S bond (0.45 versus 0.72).

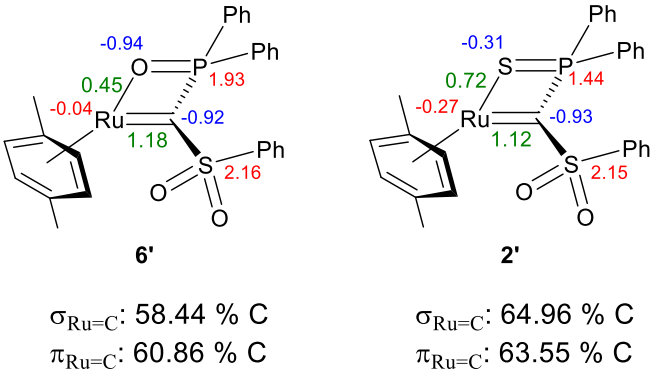

Fig. 4. Natural atomic charges (red, blue), Wiberg bond indices of the Ru═C and Ru–S/O bonds (green) and NBO analysis of **6'** and **2'** (PBE0/def2tzvp + ECP MWB28 for Ru).

3. Conclusions

In summary, a new P═O tethered methanide ligand system has been synthesized to compare its ability to form nucleophilic carbene complexes with a previously reported thiophosphoryl system. The metallated ligand was successfully isolated and used to synthesize the ruthenium chlorido complex **4** which was subsequently subjected to a dehydrohalogenation to synthesize the carbene complex **6**. Surprisingly, NMR and XRD spectroscopy revealed the product to be the cyclometallated complex **5** instead of the desired carbene complex. This is in contrast to the corresponding thiophosphoryl-substituted carbene complex **2** which was found to be stable at room temperature and showed no cyclometallation reaction. DFT studies were performed to better understand the overserved reactivity differences. The calculations revealed that the Ru═C bond in both carbene complexes is similar, thus suggesting that the cyclometallation is not the result of a higher nucleophilic character of the carbene ligand in **6**. Instead, the weaker coordination of the oxophosphoryl moiety compared to the thiophosphoryl moiety was found to enable the coordination of a C–H bond in *ortho* position of the sulfonyl bound phenyl ring to the metal centre and hence allowed the facile C–H activation at room temperature. Due to the stronger donor ability of the

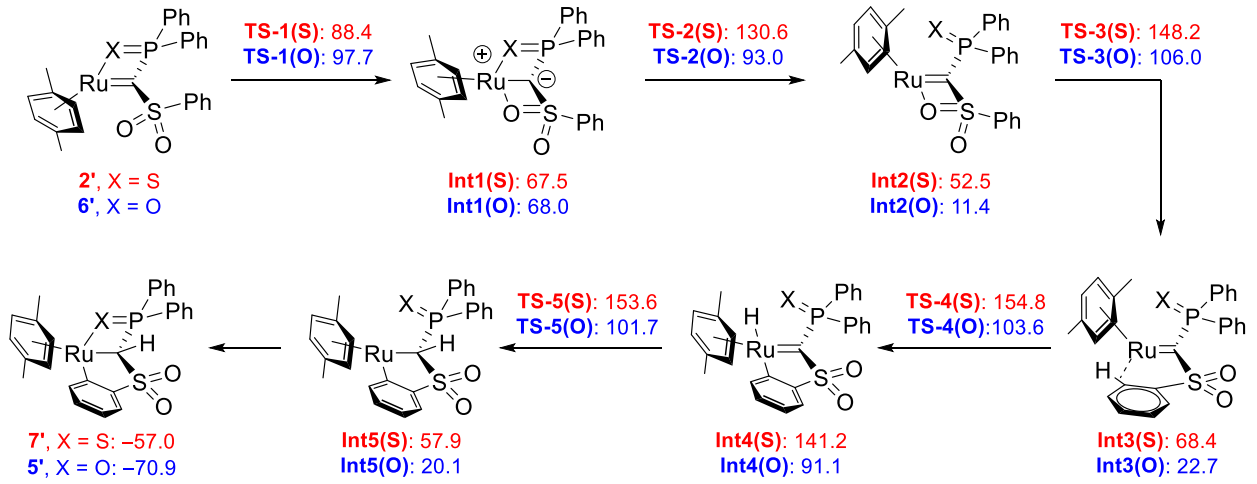

Scheme 4. Calculated pathway for the cyclometallation reactions of **2′** and **6'**; free energies are given relative to **2′** and **6′** respectively in kJ/mol [PBE0/def2tzvp + MWB28 for Ru].

thiophosphoryl moiety, the reaction barriers and intermediates of the cyclometallation process are too high in energy, thus making carbene complex **2** inert towards C–H activation. These results give valuable insights on the effects of different donor functionalities in the ligand backbone on the stability and reactivity of the corresponding carbene complexes and will be helpful for future modifying and fine-tuning of methandiide-derived carbene complexes.

4. Experimental section

4.1. General methods

All experiments were carried out under a dry, oxygen-free argon atmosphere using standard Schlenk techniques. Solvents were dried using an MBraun SPS-800. ^{1}H, ^{13}C{^{1}H}, and ^{31}P{^{1}H} NMR spectra were recorded on Avance-III–400 spectrometers at 25 °C if not stated otherwise. All values of the chemical shifts are in ppm regarding the δ-scale. All spin-spin coupling constants (J) are printed in Hertz (Hz). To display multiplicities and signal forms correctly the following abbreviations were used: s = singlet, d = doublet, t = triplet, q = quartet, sep = septet, m = multiplet, br = broad signal. Signal assignment was supported by HSQC and HMBC experiments. Elemental analyses were performed on an Elementar vario MICRO-cube elemental analyzer. All reagents were purchased from Sigma-Aldrich, ABCR, Rockwood Lithium, Acros Organics or Alfa Aesar and used without further purification, unless otherwise noted.

Synthesis of compound 3. The synthesis of **3** was achieved with an adapted procedure reported by Imamoto et al. [10] Methyl phenyl sulfone (2.00 g, 12.8 mmol) was dissolved in 40 ml THF and the solution cooled to 0 °C. *n*BuLi (5.74 ml, 12.8 mmol, 2.23 M in hexane) was slowly added in the course of 30 min. The resulting solution was stirred for 30 min. Al(*i*Bu)$_3$ (11.6 ml, 12.8 mmol, 1.1 M in toluene) was added over 30 min. The reaction mixture was stirred for additional 30 min and subsequently slowly added to a solution of ClPPh$_2$ (3.67 g, 16.64 mmol) in 40 ml THF at 0 °C. The reaction mixture was stirred for 1 h at 0 °C and 1 h at room temperature. 100 ml H_2O were carefully added, the phases separated, and the aqueous phase extracted two times with 50 ml $CHCl_3$. The organic phases were combined, dried over Na_2SO_4, filtrated and the solvent evaporated. The residue was dissolved in 50 ml THF and an excess H_2O_2 was added. The mixture was stirred overnight. 30 ml H_2O were added, the phases separated, and the aqueous phase extracted three times with DCM (50 ml). The organic phases were combined, dried over Na_2SO_4, filtrated and the solvent removed in vacuo. The resulting solid was recrystallized from hot EtOH (85 ml) to afford 2.77 g (7.81 mmol, 61%) of **3** as colorless needles. ^{1}H NMR: (400.1 MHz, $CDCl_3$): δ = 4.28 (d, $^{2}J_{HP}$ = 10.0 Hz, 2H; SCH_2P), 7.45–7.61 (m, 9H; C$H_{SPh,meta,para}$ + C$H_{PPh,meta,para}$), 7.73–7.78 (m, 4H; C$H_{PPh,ortho}$), 7.87–7.89 (m, 2H; C$H_{SPPh,ortho}$). ^{31}P{^{1}H}-NMR: (162.0 MHz, $CDCl_3$): δ = 20.2. Further spectroscopic data are in accordance with the literature [7a].

Synthesis of compound 3-Na. 1.50 g (4.21 mmol) of compound **3** and 101 mg (4.21 mmol) of NaH were suspended in 60 ml THF and the resulting reaction mixture stirred over night at room temperature until no further gas evolution was observed. The solvent was removed under reduced pressure giving **3-Na** as a colorless solid (1.77 g, 3.93 mmol, 93%). ^{1}H NMR: (400.3 MHz, DMSO-d_6): 1.74–1.80 (m, 3H; OCH$_2$CH_2), 2.58–2.64 (m, 1H; SCHP), 3.58–3.62 (m, 3H; OCH_2), 7.26–7.28 (m, 9H; C$H_{PPh,meta}$ + C$H_{SPh,meta}$), 7.67–7.71 (m, 4H; C$H_{PPh,ortho}$), 7.72–7.81 (m, 2H; C$H_{SPh,ortho}$). ^{13}C{^{1}H} NMR: (100.7 MHz, DMSO-d_6): 25.1 (OCH$_2$CH_2), 47.8 (d, $^{1}J_{CP}$ = 129.8 Hz; SCHP), 67.0 (OCH_2), 124.9 (C$H_{SPh,ortho}$), 127.3 (d, $^{3}J_{CP}$ = 11.3 Hz; C$H_{PPh,meta}$), 127.5 (C$H_{SPh,meta}$), 128.2 (C$H_{SPh,para}$), 129.0(C$H_{PPh,para}$), 131.1 (d, $^{2}J_{CP}$ = 9.02 Hz; C$H_{PPh,ortho}$), 140.6 (d, $^{1}J_{CP}$ = 107.9 Hz; C$_{PPh,ipso}$), 152.6 (C$_{SPh,ipso}$). ^{31}P{^{1}H} NMR: (162.1 MHz, DMSO-d_6): 19.7. Anal. Calcd. for $C_{19}H_{16}NaO_3PS$ + 0.75*THF: C, 61.11; H, 5.13; S, 7.41. Found: C, 60.59; H, 4.92; S, 7.45.

Synthesis of 4. 1.55 g (3.59 mmol) of methanide **3-Na** and 1.10 g (1.79 mmol) of [(*p*-cymene)RuCl$_2$]$_2$ were dissolved in 50 ml THF and the resulting mixture stirred for 16 h. The solvent was removed *in vacuo* and the orange residue dissolved in 30 ml DCM. The mixture was filtrated, the solvent removed under reduced pressure and the obtained residue recrystallized in hot toluene. Filtration and drying gave **4** as orange needles in 65% (1.46 g) yield. ^{1}H NMR (400.3 MHz, d^8-THF): 1.28 (d, $^{3}J_{HH}$ = 6.89 Hz, 6H; CH(CH_3)$_2$), 2.21 (s, 3H, CCH_3), 2.85 (sept, $^{3}J_{HH}$ = 6.73 Hz, 1H; CH(CH$_3$)$_2$), 3.81 (d, $^{2}J_{HP}$ = 2.41 Hz, 1H; SCHP), 5.75 (d, $^{3}J_{HH}$ = 6.08 Hz, 1H; CH_{Cym}), 5.84 (d, $^{3}J_{HH}$ = 5.53 Hz, 1H; CH_{Cym}), 5.88 (d, $^{3}J_{HH}$ = 5.45 Hz, 1H; CH_{Cym}), 6.12 (d, $^{3}J_{HH}$ = 5.59 Hz, 1H; CH_{Cym}), 7.06–7.22 (m, 6H; C$H_{PPh,ortho}$ + C$H_{PPh,meta}$ + C$H_{PPh,meta}$), 7.24–7.29 (m, 6H; C$H_{PPh,ortho}$ + C$H_{SPh,ortho}$ + C$H_{SPh,meta}$), 7.32–7.36 (m, 1H; C$H_{PPh,para}$), 7.41–7.46 (m, 1H; C$H_{SPh,para}$), 7.49–7.52 (m, 1H; CH$_{PPh,para}$). ^{13}C{^{1}H} NMR (100.7 MHz, d^8-THF): 18.3 (CCH_3), 21.8 (CH(CH_3)$_2$), 23.5 (CH(CH_3)$_2$), 31.6 (CH(CH$_3$)$_2$), 42.9 (d, $^{1}J_{CP}$ = 54.6 Hz; SCHP), 80.0 (CH_{Cym}), 83.1 (CH_{Cym}), 83.8 (CH_{Cym}), 88.0 (CH_{Cym}, determined from

HSQC), 94.1 (C_{Cym}), 96.4 (C_{Cym}), 127.5 ($CH_{SPh,ortho}$/$CH_{SPh,meta}$), 128.0 (d, $^2J_{CP}$ = 12.7 Hz; $CH_{PPh,ortho}$), 128.1 (d, $^2J_{CP}$ = 12.0 Hz; $CH_{PPh,ortho}$), 129.0 ($CH_{SPPh,ortho}$/$CH_{SPh,meta}$), 131.2 (d, $^3J_{CH}$ = 10.2 Hz; $CH_{PPh,meta}$), 131.8 (d, $^4J_{CP}$ = 2.52 Hz; $CH_{PPh,para}$), 132.2 ($CH_{SPh,para}$), 123.7 ($CH_{PPh,para}$), 133.5 (d, $^3J_{CP}$ = 10.1 Hz; $CH_{PPh,meta}$), 134.3 (d, $^1J_{CP}$ = 101.0 Hz; $C_{PPh,ipso}$), 145.7 ($C_{SPh,ipso}$). $^{31}P\{^1H\}$ NMR (162.1 MHz, d^8-THF): 68.3. Anal. Calcd. for $C_{29}H_{30}ClO_3PRuS$: C, 55.63; H, 4.83; S, 5.12. Found: C, 55.77; H, 4.73; S, 4.90.

Synthesis of compound 5. 150 mg (240 μmol) of **4** and 26.0 mg (240 μmol) of KO*t*Bu were dissolved in 10 ml THF and the mixture was stirred for 120 h. The solvent was removed under reduced pressure, and the residue dissolved in 20 ml toluene. The solution was filtrated twice over a 4 Å Schlenk frit with a 2 cm bed of Celite. The solvent was removed in vacuo and the residue washed once with 10 ml pentane which gave compound **5** as a pale brown solid (77.4 mg, 55%). ^1H NMR (400.3, C_6D_6): 0.88 (d, $^3J_{HH}$ = 6.88 Hz, 3H; $CH(CH_3)_2$), 1.00 (d, $^3J_{HH}$ = 6.92 Hz, 3H; $CH(CH_3)_2$), 1.63 (s, 3H; $CH(CH_3)_2$), 2.42 (sept, $^3J_{HH}$ = 6.93 Hz, 1H; $CH(CH_3)_2$), 4.67 (d, $^3J_{HH}$ = 5.72 Hz, 1H; CH_{Cym}), 4.75 (d, $^3J_{HH}$ = 5.72 Hz, 1H; CH_{Cym}), 4.83 (d, $^2J_{HP}$ = 2.80 Hz, 1H; SC*H*P), 4.96 (d, $^3J_{HH}$ = 5.77 Hz, 1H; CH_{Cym}), 5.07 (d, $^3J_{HH}$ = 5.77 Hz, 1H; CH_{Cym}), 6.78–6.83 (m, 2H; $CH_{PPh,meta}$), 6.84–6.89 (m, 2H; $CH_{PPh,para}$ + RuCCHC*H*/SCCHC*H*), 7.05–7.13 (m, 5H; $CH_{PPh,ortho}$ + $CH_{PPh,meta}$ + $CH_{PPh,para}$), 7.28–7.32 (m, 1H; RuCCHC*H*/SCCHC*H*), 7.37 (d, $^3J_{HH}$ = 7.66 Hz, 1H; RuC*H*), 7.69–7.74 (m, 2H; $CH_{PPh,ortho}$), 8.44 (d, $^3J_{HH}$ = 7.40 Hz, 1H; SC*H*). $^{13}C\{^1H\}$ NMR (100.7 MHz, C_6D_6): 18.2 (CCH_3), 22.1 ($CH(CH_3)_2$), 23.3 ($CH(CH_3)_2$), 31.2 ($CH(CH_3)_2$), 37.5 (d, $^1J_{CP}$ = 52.7 Hz; SCHP), 81.2 (CH_{Cym}), 83.5 (CH_{Cym}), 85.2 (CH_{Cym}), 86.5 (CH_{Cym}), 91.5 (C_{Cym}), 105.5 (C_{Cym}), 124.0 (SCCHCH/RuCCHCH), 124.8 (RuCCH), 127.5 (d, $^3J_{CP}$ = 12.3 Hz; $CH_{PPh,meta}$), 128.8 (d, $^3J_{CP}$ = 11.9 Hz; $CH_{PPh,meta}$), 130.2 (d, $^2J_{CP}$ = 10.1 Hz; $CH_{PPh,ortho}$), 130.5 (SCCHCH/RuCCHCH), 131.5 (d, $^4J_{CP}$ = 3.06 Hz; $CH_{PPh,para}$), 131.7 (d, $^2J_{CP}$ = 10.5 Hz; $CH_{PPh,ortho}$), 132.1 (d, $^1J_{CP}$ = 89.2 Hz; $C_{PPh,ipso}$), 132.2 (d, $^4J_{CP}$ = 2.77 Hz; $CH_{PPh,para}$), 134.3 (d $^1J_{CP}$ = 93.6 Hz; $C_{PPh,ipso}$), 142.4 (SCCH), 152.0 (SC/RuC), 167.3 (SC/RuC). $^{31}P\{^1H\}$ (162.1 MHz, C_6D_6): 61.8. Anal. Calcd. for $C_{29}H_{29}O_3PRuS$: C, 59.07; H, 4.96; S, 5.44. Found: C, 58.91; H, 4.89; S, 5.00.

X-ray crystallography. Data collection of the compounds was conducted with an Oxford Synergy. The structures were solved using direct methods, refined with the Shelx software package and expanded using Fourier techniques. **17** The crystals of all compounds were mounted in an inert oil (perfluoropolyalkylether). Crystal structure determination were affected at 100 K. Crystallographic data (excluding structure factors) have been deposited with the Cambridge Crystallographic Data Centre as supplementary publication no. CCDC 1979586-1979589. Copies of the data can be obtained free of charge on application to Cambridge Crystallographic Data Centre, 12 Union Road, Cambridge CB2 1EZ, UK; [fax: (+44) 1223-336-033; email: deposit@ccdc.cam.ac.uk].

Crystal data for compound 3. Single crystals suitable for X-ray diffraction analysis were obtained by slowly diffusing pentane in a saturated solution of **3** in THF. $C_{19}H_{17}O_3PS$: M_r = 356.35 g mol^{-1}; colourless needle; 0.13 × 0.04 × 0.03 mm^3; monoclinic; space group $P2_1/c$; a = 8.34776(18), b = 18.1226(4), c = 11.2962(2) Å; V = 1664.33(6) Å^3; Z = 4; ρ_{calcd} = 1.422 gcm^{-3}; μ = 2.759 mm^{-1}; $F(000)$ = 744; T = 100(2) K; R_1 = 0.0434 and wR_2 = 0.1112; 2981 unique reflections (θ < 67.061) and 225 parameters.

Crystal data for compound 3-Na. Single crystals suitable for X-ray diffraction analysis were obtained by slowly diffusing pentane in a saturated solution of **3-Na**+15-crown-5 in THF. $C_{29}H_{36}NaO_8PS$: M_r = 598.60 g mol^{-1}; colourless block; 0.08 × 0.15 × 0.38 mm^3; monoclinic; space group $P2_1$; a = 15.4271(4), b = 11.0281(2), c = 18.1724(4) Å; V = 2980.94(12) Å^3; Z = 4; ρ_{calcd} = 1.334 g cm^{-3}; μ = 2.020 mm^{-1}; $F(000)$ = 1264; T = 100(2) K; R_1 = 0.0284 and wR_2 = 0.0742; 8638 unique reflections (θ < 67.060) and 730 parameters.

Crystal data for compound 4. Single crystals suitable for X-ray diffraction analysis were obtained by slowly diffusing pentane in a saturated solution of **4** in toluene. $C_{60.5}H_{65.5}Cl_2O_6P_2Ru_2S_2$: M_r = 1287.73 g mol^{-1}; orange block; 0.16 × 0.10 × 0.05 mm^3; triclinic; space group P-1; a = 12.4145(4), b = 13.4350(4), c = 19.1037(5) Å; V = 2829.89(17) Å^3; Z = 2; ρ_{calcd} = 1.511 g cm^{-3}; μ = 6.819 mm^{-1}; $F(000)$ = 1321; T = 100(2) K; R_1 = 0.0224 and wR_2 = 0.0550; 100086 unique reflections (θ < 67.076) and 691 parameters.

Crystal data for compound 5. Single crystals suitable for X-ray diffraction analysis were obtained by slowly diffusing hexane in a saturated solution of **5** in toluene. $C_{36}H_{37}O_3PRuS$: M_r = 681.75 g mol^{-1}; orange block; 0.15 × 0.07 × 0.06 mm^3; triclinic; space group P-1; a = 10.9314(4), b = 12.7493(6), c = 12.8619(5) Å; V = 1508.89(12) Å^3; Z = 2; ρ_{calcd} = 1.501 g cm^{-3}; μ = 5.636 mm^{-1}; $F(000)$ = 704; T = 100(2) K; R_1 = 0.0369 and wR_2 = 0.1038; 5378 unique reflections (θ < 67.070) and 375 parameters.

Computational details. All calculations were performed without symmetry restrictions. Starting coordinates for **2′**, **5′**, **6′** and **7′** were obtained from the crystal structure analyses, for the other structures via GaussView 3.0 [18]. The geometry optimization, NBO analyses and transition state search were carried out with the Gaussian09 (Revision E.01) program package [19] using Density-Functional Theory (DFT) [20] with the PBE0 functional [21] and the def2svp basis set and the corresponding MWB28 ECP for ruthenium and the def2svp basis set [22] for all other atoms with Grimme's D3 dispersion correction with Becke-Johnson damping [23]. The metrical parameters of the energy-optimized geometry compared well with those determined by X-ray diffraction. Harmonic vibrational frequency analysis was performed on the same levels of theory to determine the nature of the structures [24]. The vibrational frequency analyses showed no imaginary frequencies for the ground states and one imaginary frequency for the transition states, corresponding to the expected translational motion of the transition states. Single point energies were calculated with the PBE0 functional and the def2tzvp basis set and the corresponding MWB28 ECP for Ruthenium and the def2tzvp basis set for all other atoms with Grimme's D3 dispersion correction with Becke-Johnson damping [12,17]. NBO analyses were performed on the same level of theory.

We calculated several other possible mechanisms for the cyclometallation process. For example, an alternative intermediate **Int1′** which features a Ru=C double bond and an η^4 coordination of the arene ligand instead is energetically highly disfavored (see SI 4.1.2). Direct transition states from the carbene complexes **2′** and **6′** to the intermediates **Int2** and **Int3**, respectively, or a direct C–H activation step via addition across the Ru–C bond could not be found. The first steps of an orthometallation at the sulfur bound phenyl ring were also investigated (see SI 4.1.3). Although this pathway features energies and barriers achievable at room temperature for complex **6′** it results in a cyclometallated compound which is significantly disfavored compared to compound **5′**. All energies, barriers and coordinates can be found in the supporting information.

Declaration of competing interests

The authors declare that they have no known competing financial interests or personal relationships that could have appeared to influence the work reported in this paper.

Acknowledgments

This work was supported by the German Research Foundation (Emmy-Noether grant DA1402/1). Gefördert durch die Deutsche Forschungsgemeinschaft (DFG) im Rahmen der Exzellenzstrategie des Bundes und der Länder – EXC 2033 – Projektnummer 390677874 – RESOLV.

Appendix A. Supplementary data

Supplementary data to this article can be found online at https://doi.org/10.1016/j.jorganchem.2020.121235.

References

[1] a) R.G. Cavell, R.P. Kamalesh Babu, A. Kasani, R. McDonald, J. Am. Chem. Soc. 121 (1999) 5805;
b) R.P. Kamalesh Babu, R. McDonald, R.G. Cavell, Chem. Commun. (2000) 481.
[2] Review articles on methandiide based carbene complexes a) N.D. Jones, R.G. Cavell, J. Organomet. Chem. 690 (2005) 5485;
b) T. Cantat, N. Mézailles, A. Auffrant, P. Le Floch, Dalton Trans. 1957 (2008);
c) S.T. Liddle, D.P. Mills, A. Wooles, J. Organomet. Chem. 36 (2010) 29;
d) S. Harder, Coord. Chem. Rev. 255 (2011) 1252;
e) T.K. Panda, P.W. Roesky, Chem. Soc. Rev. 38 (2009) 2782;
f) S.T. Liddle, D.P. Mills, A.J. Wooles, Chem. Soc. Rev. 40 (2011) 2164;
g) G.R. Giesbrecht, J.C. Gordon, Dalton Trans. (2004) 2387;
h) O.T. Summerscales, J.C. Gordon, RSC Adv. 3 (2013) 6682;
I) V.H. Gessner, J. Becker, K.-S. Feichtner, Eur. J. Inorg. Chem. (2015) 1841–1859.
[3] For examples, see a) D.P. Mills, A.J. Wooles, J. McMaster, W. Lewis, A.J. Blake, S.T. Liddle, Organometallics 28 (2009) 6771;
b) K. Aparna, M. Ferguson, R.G. Cavell, J. Am. Chem. Soc. 122 (2000) 726;
c) A.J. Wooles, O.J. Cooper, J. McMaster, W. Lewis, A.J. Blake, S.T. Liddle, Organometallics 29 (2010) 2315;
d) S.T. Liddle, J. McMaster, J.C. Green, P.L. Arnold, Chem. Commun. (2008) 1747;
e) D.P. Mills, O.J. Cooper, F. Tuna, E.J.L. McInnes, E.S. Davies, J. McMaster, F. Moro, W. Lewis, A.J. Blake, S.T. Liddle, J. Am. Chem. Soc. 134 (2012) 10047;
f) M. Fustier-Boutignon, H. Heuclin, X.F. Le Goff, N. Mézailles, Chem. Commun. 48 (2012) 3306;
g) M. Gregson, E. Lu, J. McMaster, W. Lewis, A.J. Blake, S.T. Liddle, Angew. Chem. 125 (2013) 13254;
h) M. Fustier, X.F. Le Goff, P. Le Floch, N. Mézailles, J. Am. Chem. Soc. 132 (2010) 13108;
i) T. Cantat, M. Demange, N. Mézailles, L. Ricard, Y. Jean, P. Le Floch, Organometallics 24 (2005) 4838;
j) T. Cantat, N. Mézailles, L. Ricard, Y. Jean, P. Le Floch, Angew. Chem. Int. Ed. 43 (2004) 6382;
k) T. Cantat, X. Jacques, L. Ricard, X.F. Le Goff, N. Mézailles, P. Le Floch, Angew. Chem. Int. Ed. 46 (2007) 5947;
l) T. Cantat, F. Jaroschik, L. Ricard, P. Le Floch, F. Nief, N. Mézailles, Organometallics 25 (2006) 1329;
m) T. Cantat, F. Jaroschik, F. Nief, L. Ricard, N. Mézailles, P. Le Floch, Chem. Commun. (2005) 5178;
n) E. Lu, O.J. Cooper, J. McMaster, F. Tuna, E.J.L. McInnes, W. Lewis, A.J. Blake, S.T. Liddle, Angew. Chem. Int. Ed. 53 (2014) 6696;
o) E. Lu, W. Lewis, A.J. Blake, S.T. Liddle, Angew. Chem. Int. Ed. 53 (2014) 9356.
[4] For reviews, see (a) V.K.K. Praneeth, M.R. Ringenberg, T.R. Ward, Angew. Chem. 124 (2012) 2;
(b) O.R. Luca, R.H. Crabtree, Chem. Soc. Rev. 42 (2013) 1440;
(c) H. Grützmacher, Angew. Chem. Int. Ed. 47 (2008) 1814;
(d) J.I. van der Vlugt, J.N.H. Reek, Angew. Chem. Int. Ed. 48 (2009) 8832;
(e) S. Schneider, J. Meiners, B. Askevold, Eur. J. Inorg. Chem. (2012) 412;
(f) V. Lyaskovskyy, B. de Bruin, ACS Catal. 2 (2012) 270;
(g) J. Khusnutdinova, D. Milstein, Angew. Chem. Int. Ed. 54 (2015) 12236.
[5] a) D.V. Gutsulyak, W.E. Piers, J. Borau-Garcia, M. Parvez, J. Am. Chem. Soc. 135 (2013) 11776;
b) J. Becker, T. Modl, V.H. Gessner, Chem. Eur J. 20 (2014) 11295;
c) J. Weismann, V.H. Gessner, Chem. Eur J. 21 (2015) 16103;
d) J. Weismann, V.H. Gessner, Chem. Commun. 51 (2015) 14909;
e) J. Weismann, L.T. Scharf, V.H. Gessner, Organometallics 35 (2016) 2507;
f) L.T. Scharf, J. Weismann, K.-S. Feichtner, V.H. Gessner, Chem. Eur J. 24 (2018) 3439;
g) A.V. Polukeev, O.F. Wendt, Organometallics 36 (2017) 639.
[6] K.-S. Feichtner, V.H. Gessner, Chem. Commun. 54 (2018) 6540.
[7] a) J. Becker, V.H. Gessner, Organometallics 33 (2014) 1310;
b) J. Weismann, V.H. Gessner, Eur. J. Inorg. Chem. (2015) 4192;
c) K.-S. Feichtner, S. Englert, V.H. Gessner, Chem. Eur J. 22 (2016) 506;
d) J. Weismann, R. Waterman, V.H. Gessner, Chem. Eur J. 22 (2016) 3646;
e) K.-S. Feichtner, T. Scherpf, V.H. Gessner, Organometallics 37 (2018) 645.
[8] For further phosphoryl-substituted methandiide complexes, see a) H. Heuclin, D. Grünstein, X.-F. Le Goff, P. Le Floch, N. Mézailles, Dalton Trans. 39 (2010) 492;
b) J.F.K. Müller, K.J. Kulicke, M. Neuburger, M. Spichty, Angew. Chem. Int. Ed. 40 (2001) 2890;
c) H. Heuclin, M. Fustier-Boutignon, S.Y.-F. Ho, X.-F. Le Goff, S. Carenco, C.-W. So, N. Mézailles, Organometallics 32 (2013) 498.
[9] V.H. Gessner, F. Meier, D. Uhrich, M. Kaupp, Chem. Eur J. 19 (2013) 16729.
[10] T. Imamoto, K. Hiroyasu, Synthesis 10 (1985) 982.
[11] K.-S. Feichtner, V.H. Gessner, Inorganics 4 (2016) 40.
[12] G. Boche, Angew Chem. Int. Ed. Engl. 28 (1989) 277.
[13] P. Schröter, V.H. Gessner, Chem. Eur J. 18 (2012) 11223.
[14] a) T. Cantat, M. Demange, N. Mézailles, L. Ricard, Y. Jean, P. Le Floch, Organometallics 24 (2005) 4838–4841;
b) H. Heuclin, X.F. Le Goff, N. Mézailles, Chem. Eur J. 18 (2012) 16136–16144;
c) N.D. Jones, G. Lin, R.A. Gossage, R. McDonald, R.G. Cavell, Organometallics 22 (2003) 2832–2841.
[15] Gaussian NBO Version 3.1, Glendening, E. D.; Reed, A. E.; Carpenter, J. E.; Weinhold, F..
[16] It is noteworthy, that both complexes show WBIs higher than 1 indicating a considerable double bond character. Carbene Complexes with "True" Metal Carbon Double Bonds Usually Exhibit WBIs between 1 and 1.5, Ylidic Metal Carbon Interactions or Single Bonds Show WBIs Considerably Lower than 1. See Reference 9 for Details. For Example: the WBIs of the Ru–C Bonds in the Corresponding Orthometallated Compounds **5'** and **7'**amount to 0.6301 and 0.6371, respectively.
[17] a) G. Sheldrick, Acta Crystallogr. A: Found. Crystallogr. A64 (2008) 112–122;
b) G. Sheldrick, Acta Crystallogr. A71 (2015) 3;
c) CrysAlisPro, Agilent Technologies, Version 1.171.36.24 (release 03-12-2012 CrysAlis171 .NET) (compiled Dec 3 2012, 18:21:49). d) CrysAlisPro 1.171.38.43, Rigaku OD, 2015.
[18] GaussView, Gaussian, Inc., Pittburgh PA, 2000. Version 3.0.
[19] Gaussian 09, Revision E.01 M.J. Frisch, G.W. Trucks, H.B. Schlegel, G.E. Scuseria, M.A. Robb, J.R. Cheeseman, G. Scalmani, V. Barone, B. Mennucci, G.A. Petersson, H. Nakatsuji, M. Caricato, X. Li, H.P. Hratchian, A.F. Izmaylov, J. Bloino, G. Zheng, J.L. Sonnenberg, M. Hada, M. Ehara, K. Toyota, R. Fukuda, J. Hasegawa, M. Ishida, T. Nakajima, Y. Honda, O. Kitao, H. Nakai, T. Vreven, J.A. Montgomery Jr., J.E. Peralta, F. Ogliaro, M. Bearpark, J.J. Heyd, E. Brothers, K.N. Kudin, V.N. Staroverov, T. Keith, R. Kobayashi, J. Normand, K. Raghavachari, A. Rendell, J.C. Burant, S.S. Iyengar, J. Tomasi, M. Cossi, N. Rega, J.M. Millam, M. Klene, J.E. Knox, J.B. Cross, V. Bakken, C. Adamo, J. Jaramillo, R. Gomperts, R.E. Stratmann, O. Yazyev, A.J. Austin, R. Cammi, C. Pomelli, J.W. Ochterski, R.L. Martin, K. Morokuma, V.G. Zakrzewski, G.A. Voth, P. Salvador, J.J. Dannenberg, S. Dapprich, A.D. Daniels, O. Farkas, J.B. Foresman, J.V. Ortiz, J. Cioslowski, D.J. Fox, Gaussian, Inc., 2013. Wallingford CT.
[20] a) P. Hohenberg, W. Kohn, Phys. Rev. 136 (1964) B864;
b) W. Kohn, L.J. Sham, Phys. Rev. 140 (1965) A1133.
[21] C. Adamo, V. Barone, J. Chem. Phys. 110 (1999) 6158.
[22] a) D. Andrae, U. Häußermann, M. Dolg, H. Stoll, H. Preuß, Theor. Chim. Acta 77 (1990) 123;
b) F. Weigend, R. Ahlrichs, Phys. Chem. Chem. Phys. 7 (2005) 3297.
[23] a) S. Grimme, J. Antony, S. Ehrlich, H. Krieg, J. Chem. Phys. 132 (2010) 154104;
b) S. Grimme, S. Ehrlich, L. Goerigk, J. Comput. Chem. 32 (2011) 1456;
c) D.G.A. Smith, L.A. Burns, K. Patkowski, C.D. Sherrill, J. Phys. Chem. Lett. 7 (2016) 2197.
[24] P. Deglmann, F. Furche, R. Ahlrichs, Chem. Phys. Lett. 362 (2002) 511.